Int. J. Solids Structures Vol. 27, No. 6, pp. 783–808, 1991
Printed in Great Britain.

0020-7683/91 $3.00+.00
Pergamon Press plc

LINEAR STABILITY ANALYSIS OF RATE-DEPENDENT DISCRETE SYSTEMS

YVES M. LEROY
Koninklijke/Shell Exploratie en Produktie Laboratorium (Shell Research BV), Rijswijk, The Netherlands

(*Received* 13 *October* 1989; *in revised form* 12 *April* 1990)

Abstract—The analysis of a Shanley column is first presented, in order to illustrate the role of rate dependence in the uniqueness of and stability conditions for the solution of the discrete system. Stability conditions for the solution of boundary-value problems for rate-dependent solids are then considered, and a weak formulation of the linear stability criterion is presented. This formulation is well-suited for obtaining solutions to both the instability modes and the corresponding critical loads in systems with a finite number of degrees of freedom, typically obtained by discretization of the continuum. As an application, a stability analysis by the finite-element method of a von Mises solid under plane strain tensile loading is presented. The influence of both the rate sensitivity and the wavelength of the mode of perturbation on the subsequent localization of the deformation in shear bands is discussed.

1. INTRODUCTION

Localization of the deformation is a characteristic feature of inelastic deformation and has been studied extensively for rate-independent solids within the context of bifurcation theory. The onset of localization can be characterized by different modes of bifurcation such as necking modes (Hill and Hutchinson, 1975), surface wave modes (Triantafyllidis, 1980) or bands of intense shearing (Rice, 1976; Hutchinson and Tvergaard, 1981). Bifurcation is understood in this paper as a loss of uniqueness in the solution of the incremental governing equations. Loss of uniqueness, which is either associated with or can be followed by a change in character of the governing equations, is responsible for standard boundary-value problems becoming ill-posed. For example, within the theoretical framework of Hadamard (1903), the initiation of shear banding under quasi-static conditions is signalled by a loss of ellipticity and the characteristics of the hyperbolic system define the orientation of the shear bands.

For rate-dependent solids, conditions for the uniqueness and the existence of the solution of incremental governing equations have been studied by Mandel (1971). An example of interest is the case of materials that exhibit no instantaneous permanent deformation and for which the elastic component of the constitutive model solely controls conditions for uniqueness. In general, for stress levels that remain small compared with the elastic stiffnesses, uniqueness in the solution of the incremental governing equations is guaranteed. Boundary-value problems then remain well-posed and bifurcation is precluded in the loading range for which localization phenomena are observed (Needleman, 1988). Changes in the mode of deformation, which typically precede a localization of the deformation, can be detected by a linear stability analysis. A solution is said to be unstable if the analysis reveals the growth of a potential infinitesimal perturbation.

Localization phenomena in strain-rate-dependent materials are well illustrated in the experimental work of Marchand and Duffy (1988), in which the dynamic loading of a thin-walled cylinder in a torsional Kolsky bar results in shear banding. A simple equivalent model problem could be one characterized initially by homogeneous deformation in simple shear. The deformation ceases to be homogeneous at some point of the loading owing to the growth of a small perturbation. The final localization in a narrow band of intense shearing is characterized by an unbounded growth of the initially small perturbation. The stability of the homogeneous mode of deformation in simple shear was first analysed by Clifton (1978) and Bai (1982), accounting for temperature effects and considering linear

perturbation methods. An extension of these studies to three dimensions was proposed by Anand *et al.* (1987).

Stability analyses based on linear perturbation methods aim at predicting the initial evolution of the perturbations and usually fail to reveal the long-term evolution during which localization could take place. Localization is detected when the rate of growth of the perturbation becomes large compared with the variation of the fundamental solution, which is disregarded in a linear analysis. A localization criterion necessitates a relative perturbation analysis, such as can be found in the work of Molinari and Clifton (1987).

The two concepts of uniqueness and stability are first discussed in this paper in the context of the analysis of a discrete system with two degrees of freedom, the Shanley column. The supports of the column are considered to have an elastic–viscoplastic response. Whereas uniqueness in the solution of the incremental governing equations for a perfect column is lost at the Euler buckling load under quasi-static conditions, the onset of an unstable behaviour is observed for a lower load level. More precisely, buckling initiates for a critical load governed by the tangent modulus that characterizes the limit of inviscid plastic flow. An analogous approach to stability for rate-dependent solids is then considered, and a weak formulation of the linear stability criterion is presented. The aim here is to find both the stability threshold and the associated mode for systems with a finite number of degrees of freedom. These systems are typically obtained by discretization of the continuum. As an application, the stability analysis by the finite-element method of a von Mises solid under plane strain tensile loading is presented. The modes of bifurcation for the rate-independent solid are known to be of the wave or shear-band mode (Hill and Hutchinson, 1975) and correspond to the modes of instability of the rate-dependent solid. The final failure mechanism is one of shear banding. Both the influence of the rate sensitivity and the perturbation wavelength on the development and the final position of the shear bands on the specimen are discussed. A convergence analysis shows the sensitivity of the simulation of the localization phenomenon to the mesh size.

2. STABILITY ANALYSIS OF A SHANLEY COLUMN

In this section, the stability analysis of a Shanley column with elastic–viscoplastic response is presented. The development of the rotation during the buckling of the slender column is a typical example of the growth of an infinitesimal perturbation in the principal mode of deformation, defined here by the loading of a straight column that remains untilted. The analysis of this discrete system will shed light on the analysis of analogous continuous systems and thus offers an ideal opportunity to review classical results on uniqueness within a simple framework.

Models of slender column analogous to the one treated here and presented in Figs 1a and 1b have been studied repeatedly in the literature, starting with Shanley's (1947) successful attempt to reconcile buckling load predictions based on tangent modulus and reduced modulus. A complete analysis of the elastoplastic column using static perturbation techniques was presented by Sewell (1965). Within the framework of standard systems, Nguyen (1984) re-examined the stability and the bifurcation criteria for the same structure. The sensitivity to imperfections of the post-buckling response of a similar elastoplastic column was investigated by Hutchinson (1972). For stability analyses of viscoplastic columns, one should mention the contributions of Rabotnov and Shesterikov (1957) and Hoff (1958) in the special context of creep buckling. In these last two works, the stability analysis is carried out on the dynamic system of a prestressed column subjected to a perturbing impulse. Owing to the non-linear material response, such an impulse results in the initiation of buckling beyond a critical time, which defines the stability threshold. In this paper the approach to column stability is different. The impulse type of analysis is replaced by classical linear perturbation techniques. Furthermore, an elastic–viscoplastic constitutive model is considered for the column supports. This choice permits a comparison with rate-independent behaviour in the limit of inviscid plastic flow.

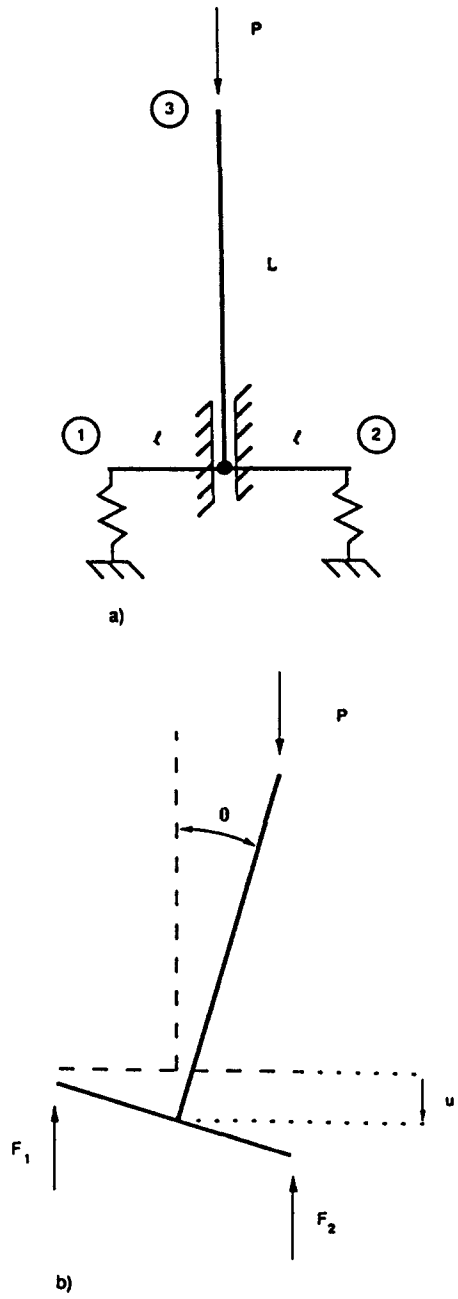

Fig. 1. Geometry and free body diagram of the Shanley column.

2.1. *Governing equations and uniqueness conditions*

The equations of motion for the rigid rod model presented in Fig. 1 are:

$$F_1 + F_2 - P = m\ddot{u}_G$$
$$(F_1 - F_2)l + PL\theta = I\ddot{\theta}, \tag{1}$$

where m is the total mass of the column, u_G the vertical displacement of the centre of gravity and I the moment of inertia with respect to the centre of rotation. The forces F_1 and F_2 are associated with the generalized springs labelled 1 and 2 on Fig. 1, and P is the applied load on the top of the column, labelled 3. The compatibility equations relate the displacement

of each support to the two degrees of freedom of the system, the vertical displacement u of the constrained centre and the rotation θ:

$$u_\alpha = u + l_\alpha \theta, \quad \alpha = 1, 2. \tag{2}$$

In this equation, l_α is the distance from support α to the centre of rotation: $l_\alpha = (-l, +l)$. As a convention in this section, there is no summation over repeated Greek subscripts, which range from 1 to 2. The vertical displacement of the centre of gravity is expressed as a convex combination of the displacement u of the column centre and the top displacement u_3:

$$u_G \equiv (1-\beta)u + \beta u_3 = u + \beta \frac{L}{2}\theta^2, \quad \beta \in [0; 1]. \tag{3}$$

Note that the coefficient β will have no influence on the results to be presented in this section.

We now consider a class of elastic–viscoplastic constitutive models for the supports, described by the following set of equations:

$$\begin{aligned} \dot{F}_\alpha &= E(\dot{u}_\alpha - \dot{u}^p_\alpha) \\ \dot{u}^p_\alpha &= \frac{\phi(F_\alpha, F_{0\alpha})}{\eta} \quad \text{if} \quad F_\alpha \geqslant F_{0\alpha}, \quad \text{zero otherwise} \\ F_{0\alpha} &= F_0(u^p_\alpha). \end{aligned} \tag{4}$$

The permanent displacement rate of each support is denoted by $\dot{u}^p_\alpha$, while E, η and $F_0(u^p_\alpha)$ are respectively the elastic stiffness, a viscosity, and a hardening function of the accumulated permanent displacement. The function ϕ characterizes a general viscosity law with the only restriction that this function is zero for F_α less than $F_{0\alpha}$, corresponding in this range to an elastic response of the supports.

The boundary conditions at the top of the column can be specified in terms of either force or displacement:

$$\begin{aligned} u_3 &= u + \frac{L}{2}\theta^2 = \bar{U}(t) \\ P &= \bar{P}(t). \end{aligned} \tag{5}$$

Note that in eqns (1)–(3) and (5) the rotation θ of the column is assumed to remain small throughout the analysis. A solution to the set of eqns (1)–(4) together with either (5a) or (5b) can be obtained, and at any time the state of the column is characterized by the set of variables $(F_\alpha, P, u, u^p_\alpha, u_G, \theta)$. In particular, we shall call the *fundamental* or *principal solution* of this problem the path corresponding to an initially straight column that remains untilted: $(F^0_\alpha, P^0, u^0, u^{p0}_\alpha, u^0_G, 0)$.

Considering now the uniqueness of this principal solution, we follow the standard approach and allow for the possibility of having a second family of incremental variables $(\dot{F}_\alpha, \dot{P}, \dot{u}, \dot{u}^p_\alpha, \dot{u}_G, \dot{\theta})$ satisfying governing equations and boundary conditions, and which differs from the incremental fundamental solution. The difference between the two families of incremental solutions is denoted by Δ. From the constitutive equations (4) it is seen that the permanent displacement rates $\dot{u}^p_\alpha$ depend only on the current values of F_α and $F_{0\alpha}$ and that consequently the traction and displacement rate differences are simply related by the elastic modulus:

$$\Delta \dot{F}_z = E\Delta \dot{u}_z. \tag{6}$$

By inserting (6) in the rate form of the governing eqns (1)–(3), the uniqueness problem for the rotation is found to be governed by the single equation:

$$(P(t)L - 2EI^2)\Delta\dot{\theta} - I\Delta\ddot{\theta} = 0. \tag{7}$$

In the absence of inertia, it can be concluded from (7) that a loss of uniqueness is associated with the Euler buckling load $P_E = 2EI^2/L$. Under dynamic conditions, the result is different. Solutions of (7) can be approximated, on a time interval that is small compared with the rate of loading, by trigonometric functions for applied loads below the Euler load and by hyperbolic functions otherwise. Furthermore, uniqueness of the solution of (7) can be proved by applying the Lipschitz condition (Coddington and Levinson, 1955) to the system of two first-order equations with the unknowns $(\Delta\dot{\theta}, \Delta\ddot{\theta})$ obtained from (7). Consequently, if uniqueness is ensured initially $[(\Delta\dot{\theta}, \Delta\ddot{\theta})|_{t=0} = (0, 0)]$, then by continuity requirement this initial trivial solution remains the only admissible solution at any time. The introduction of inertia terms ensures uniqueness of the solution of the incremental governing equations beyond the Euler load.

We may conclude from this analysis that the Shanley column problem is well-posed up to the Euler load under quasi-static conditions and that it remains so for any load level, if inertia is taken into account. We must now answer the question of whether or not the unique solution along the fundamental path will exist physically. To determine the physical existence of the solution, a stability analysis is required.

2.2. *Stability analysis*

To investigate the asymptotic stability in the Lyapunov sense (Coddington and Levinson, 1955; Arnold, 1973) of the principal solution, we now assume that at a given time there exist solutions, called perturbed solutions, in the neighborhood of the fundamental solution. Stability is guaranteed as long as the distance between any such admissible perturbed solution and the fundamental one is found to vanish with time, for some appropriate definition of a distance.

The existence of perturbed solutions neighbouring the principal solution is first explored by considering solution at time $\tau = t + \Delta t$, for Δt small compared to unity, of the type:

$$A(\tau) = A^0(\tau) + \varepsilon\delta A(\tau) \quad \text{with} \quad \varepsilon \ll 1, \tag{8}$$

where A is generic for all field quantities (F_z, P, u, u_z^p, u_G, θ) and $A^0(\tau)$ characterizes the principal solution at time τ. For such a perturbed state to be admissible, it has to satisfy the field eqns (1)–(4) and the boundary condition (5a) or (5b). Substitution of (8) in these equations results in two problems of different order. The zero-order problem describes the principal solution at time τ and does not yield any information concerning the perturbations. The first-order problem, however, yields the following system:

$$\begin{aligned}
&\delta F_1(\tau) + \delta F_2(\tau) - \delta P(\tau) = m\delta\ddot{u}(\tau)\\
&(\delta F_1(\tau) - \delta F_2(\tau))l + P^0(\tau)L\delta\theta(\tau) = I\delta\ddot{\theta}(\tau)\\
&\delta u_z(\tau) = \delta u(\tau) + l_z\delta\theta(\tau)\\
&\delta\dot{F}_z(\tau) = E(\delta\dot{u}_z(\tau) - \delta\dot{u}_z^p(\tau))\\
&\eta\delta\dot{u}_z^p = \left.\frac{\partial\phi}{\partial F_z}\right|^0 \delta F_z(\tau) + \left.\frac{\partial\phi}{\partial F_{0z}}\right|^0 \delta F_{0z}(\tau)\\
&\delta F_{0z}(\tau) = F_0'(u_z^p)|^0\delta u_z^p,
\end{aligned} \tag{9}$$

together with the boundary condition:

$$\delta u(\tau) = 0 \quad \text{or} \quad \delta P(\tau) = 0. \tag{10}$$

Note that the trivial first-order relation obtained from (3) has been introduced directly into (9a). The following separation of variables is now proposed for solving the first-order problem:

$$\delta A(\tau) = \delta \hat{A} \exp(\lambda \Delta t), \tag{11}$$

where the parameter λ is the initial rate of growth of the perturbations and $\delta \hat{A}$ a scalar quantity that will remain undetermined in this linear stability analysis. This type of solution should yield an accurate estimate of the evolution of the perturbation over a time interval for which the rate of change of the perturbation is large compared with the variations in (9) of the coefficients determined by the principal solution. If a solution of (9)–(10) with structure (11) can be found such that the rate λ is positive, then a perturbation can grow. Alternatively, if the satisfaction of (9)–(10) requires negative rates of growth, the perturbation is decaying in time and initiation of buckling is precluded at time τ.

The limiting process of Δt tending to zero is now considered and the first-order problem is solved for a solution having the structure defined in (11). As a first step, a relation between the perturbations in force and displacement is derived from (9d)–(9f):

$$\delta \hat{F}_\alpha = E_\alpha(\lambda) \delta \hat{u}_\alpha$$

$$E_\alpha(\lambda) = E \Bigg/ \left(1 + E \frac{\left.\dfrac{\partial \phi}{\partial F_\alpha}\right|^0}{\lambda \eta - \left(\left.\dfrac{\partial \phi}{\partial F_{0\alpha}}\right|^0 F'_{0\alpha} \right)} \right). \tag{12}$$

The modulus $E_\alpha(\lambda)$ is a function of material parameters, the current state of deformation on the principal branch and the rate of growth of the perturbation. Note that it is not associated with the instantaneous response of the column, unlike the modulus found during the preceding uniqueness analysis. The original system (9) can now be further reduced to:

$$[E_1(\lambda) + E_2(\lambda) - m\lambda^2] \delta \hat{u} = \delta \hat{P}$$

$$[P^0(\tau) L - I^2 (E_1(\lambda) + E_2(\lambda)) - I\lambda^2] \delta \hat{\theta} = 0, \tag{13}$$

together with $\delta \hat{u} = 0$ or $\delta \hat{P} = 0$ from the boundary conditions. Since we have considered an initially perfect structure, the two supports have experienced the same deformation up to time τ and their moduli are thus identical and are denoted from now on by $\mathscr{E}(\lambda)$. At time τ, a necessary condition for the existence of a non-trivial solution in terms of a perturbation in the angular position of the column reads:

$$P^0(\tau) = 2 \frac{I^2}{L} \mathscr{E}(\lambda) + \frac{I}{L} \lambda^2. \tag{14}$$

Note that this result is independent of the choice of type of boundary condition. Equations (12b) and (14) define a one-to-one relation between the load carried by the column and the initial rate of growth of the instability. If, for a given load, the rate λ is found to be positive, then the principal solution is said to be unstable and buckling is possible.

We now analyse stability criterion (14), disregarding the contribution of inertia for the time being. From a consideration of the limit of infinite initial rate of growth ($\lambda \to \infty$) for the perturbations, it can be seen from (12b) that the modulus $\mathscr{E}$ tends to the elastic stiffness E and that the corresponding critical load defined in (14) approaches the Euler buckling load. This result indicates that whereas a loss of uniqueness is not possible before the Euler

load is reached, this load level is not attainable following the principal branch owing to the highly unstable character of this loading path. It is of more interest to determine the instability threshold corresponding to the first positive rate of growth ($\lambda \to 0^+$). Note that, to remain within the domain of validity of the linear stability analysis with a solution having the structure (11), this process requires that a vanishing loading rate be considered as well. From (12b), it follows that the first instability corresponds to the modulus:

$$\mathscr{E}_T = E \Bigg/ \left(1 - E \frac{\left.\dfrac{\partial \phi}{\partial F_x}\right|^0}{\left.\left(\dfrac{\partial \phi}{\partial F_{0\alpha}} F'_{0\alpha}\right)\right|^0} \right). \tag{15}$$

Interestingly enough, the same modulus is obtained from (12b) if the limit of inviscid plastic flow is considered ($\eta \to 0$). In this limit of inviscid plastic flow, the constitutive model (3) yields a rate-independent model in which the viscosity law is replaced by the yield criterion: $\phi(F_x, F_{0\alpha}) = 0$. The modulus $\mathscr{E}_T$ pertinent to the instability threshold represents the tangent modulus of this rate-independent model. The critical load for the first instability is associated with the tangent modulus and naturally yields a lower bound for all possible buckling loads.

To complete this discussion of criterion (14), we note the stabilizing effect of inertia. At any given load level, the rate of growth is lowered when inertia is accounted for. At the Euler load, for example, the rate of growth is found to be infinite under quasi-static conditions and bounded if inertia terms are introduced.

At this point, it is of interest to compare further the results of the linear stability analysis with the bifurcation analysis of the rate-independent column. This comparison is valid when the limit of inviscid plastic flow is considered in the preceding analysis. The explicit introduction of time in the viscoplastic model enables one to quantify the unstable character of the principal branch by assigning to every load a characteristic rate of growth of the perturbation. A further advantage of introducing viscosity effects lies in the choice of the modulus during the stability analysis. For rate-independent models and within the plastic regime, two possible moduli are always present, these corresponding to the elastic and to the plastic branches of the plasticity model. Hence it is always necessary to decide which modulus is most appropriate to the bifurcation analysis. The introduction of a small but finite viscosity obviates this discussion altogether. If plastic flow is taking place at time t, then the viscosity effects ensure the existence of a finite time interval during which plastic flow will continue even if the loading on one of the supports is reversed. This determines uniquely the modulus pertinent to the first instability as being the tangent modulus. This feature of the stability analysis of the rate-dependent system could explain the different result of the stability analysis of the elastoplastic column, corresponding to the singular limit of ($\eta = 0$), for which the stability threshold is found to be associated with the reduced modulus (Nguyen, 1984). As a consequence, the path on the principal branch beyond the first bifurcation point, corresponding to the tangent modulus, is found to be initially stable. This difference between bifurcation and stability is a rather common aspect of elastoplastic models.

2.3. *Development of the instability*

In the preceding section, the existence of admissible solutions neighbouring the fundamental one was established. Every load beyond the critical load based on the tangent modulus was found to correspond to a perturbation with a positive initial rate of growth λ. We now intend to explore the evolution of these perturbed solutions. If growth is observed, then the loss of stability predicted by the linear analysis is confirmed and buckling is taking place. This post-buckling analysis is conducted numerically in the spirit of the finite-element analysis presented in the last section of this paper.

We consider a constitutive model similar to (4) with the following particular choice of a linear overstress viscosity law and linear hardening function:

$$\dot{u}_z^p = \frac{F_z - F_{0\alpha}}{\eta} \quad \text{for} \quad F_z \geq F_{0\alpha}, \quad \text{zero otherwise}$$

$$F_{0\alpha} = F_y(1 + h u_z^p), \tag{16}$$

where F_y is the initial yield strength of a support and h is a hardening parameter. Values of 10^{-4} N and 10^3 m^{-1} were chosen for these two quantities, while the geometry of the column was defined by assigning a value of 1 m and 4×10^{-2} m to L and l. For this choice of material and geometrical parameters, relation (14) between the rate of growth of the perturbation and the load carried by the column under quasi-static conditions takes the form shown in Fig. 2 for various values of viscosity. Note that all curves start from the same critical load determined by the tangent modulus δ_T, and tend towards the Euler load as λ increases to infinity. For boundary condition (5a), the displacement at the top of the column is defined as a linear function of time: $\bar{U}(t) = \bar{v}t$, with $\bar{v}$ set to 10^{-7} m s^{-1} in this analysis.

Quasi-static conditions are assumed and an implicit numerical scheme is chosen to solve the governing eqns (1)–(4). For the critical load corresponding to a selected rate of growth, the system is perturbed by assigning a small non-zero value $\Delta\theta_1$ to the first iteration of the next incremental rotation. Figure 3 presents the history of the computed load normalized by the elastic buckling load versus a dimensionless time, normalized by the relaxation time t_R defined as $t_R \equiv \eta/E$. The instant at which the system is perturbed is marked by a solid point. The corresponding evolution of the angle θ is presented in Fig. 4. These figures show very clearly that there is a latency between the instant of perturbation and the first appearance of a significant deviation from the fundamental path. This delay

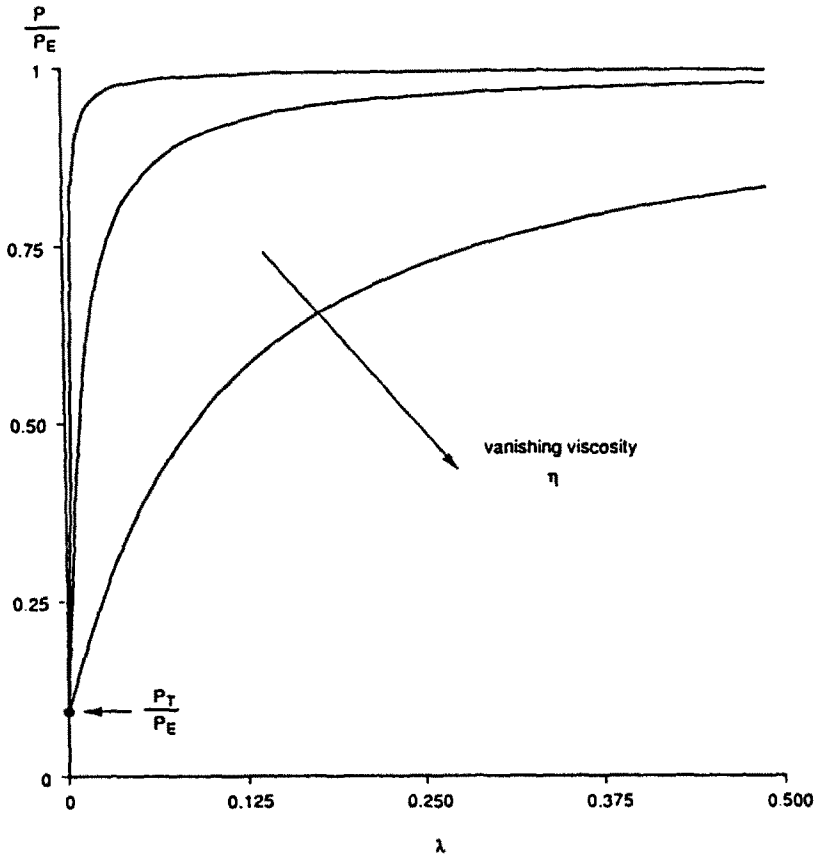

Fig. 2. Relation between the load and the initial rate of growth of the perturbation for the fundamental solution. Various choices of viscosity η are considered in the quasi-static case.

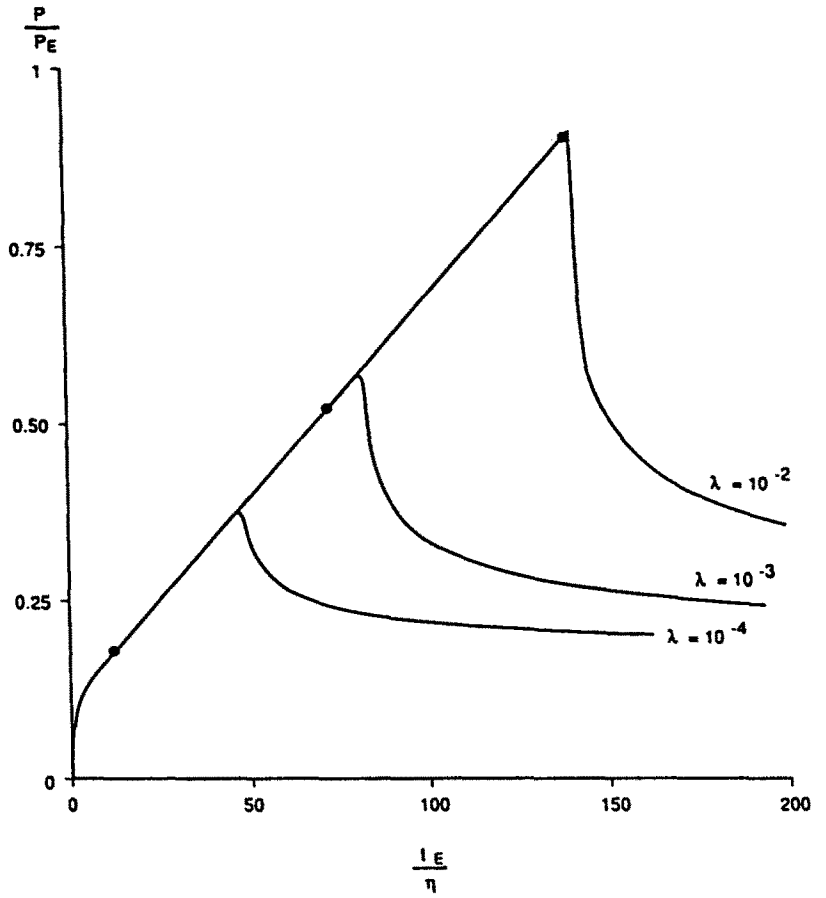

Fig. 3. Evolution of the load with time including the post-buckling regime. The analysis is performed for three different predefined rates of growth λ and the points signal the instants of perturbation.

becomes shorter for larger values of λ. After this initial period, buckling is characterized by a loss of bearing capacity of the column followed by a stabilization at a lower level. The computed column response shows the limitation of any linearized theory for predicting the long-term evolution of the perturbed system. A similar observation has already been made by Hoff (1958) in the context of creep buckling.

To compare the evolution of the solutions in the post-buckling regime with the prediction of the linear analysis, we now focus on the initial growth of the instability. The evolution of the rotation θ up to 50 times the magnitude of the perturbation $\Delta\theta_1$ is shown in Fig. 5 for various rates λ. The initial jump in θ from the horizontal axis marks the first equilibrium point away from the principal branch after perturbation. The linear stability analysis predicts a rate of growth at the time of perturbation of $\lambda\delta\hat{\theta}$. By analogy, we can estimate that in this numerical analysis the initial rate of growth should be of the order of $\lambda\Delta\theta_n$, where $\Delta\theta_n$ is the rotation found at the end of the first increment when equilibrium has been restored after n iterations. These estimates, corresponding to the dashed lines in Fig. 5, are found to be rather representative of the initial angular response, but again are unable to represent the longer-term evolution. Although the role of the parameter λ has been already established, this linear analysis cannot shed any light on the role of the magnitude of the perturbation $\delta\hat{\theta}$. From the structure of the solutions (11), it is apparent that $\delta\hat{\theta}$ contributes to the initial rate of growth of the perturbation for non-vanishing rates λ. A question to be considered at this point is whether the initial guess $\Delta\theta_1$ introduced at the time of perturbation plays the same role in the numerical analysis. To assess the sensitivity of the post-buckling analysis to this parameter, numerical tests were performed

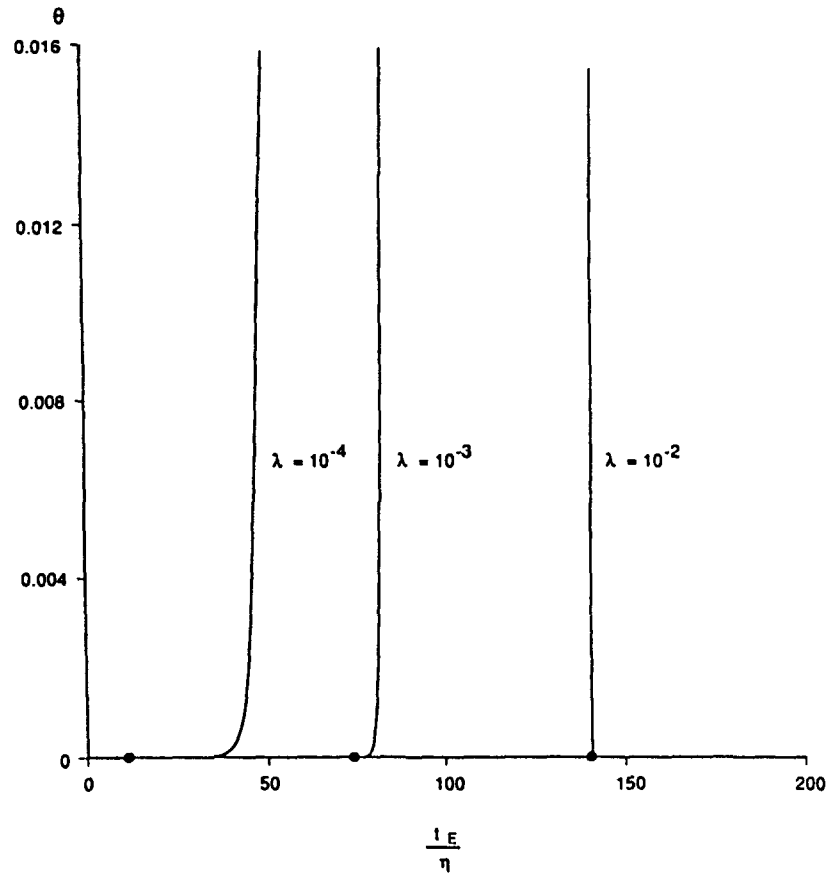

Fig. 4. Evolution of the angular position of the column θ with respect to time for three different perturbations marked by solid points.

for initial perturbations $\Delta\theta_1$ of 10^{-7} and below, and for a rate λ of the order of the rate of loading $\bar{v}/L$ of $10^{-7}\,s^{-1}$. No influence of $\Delta\theta_1$ on the evolution of the angle θ and the load P was detectable after a few increments. This result is certainly due to the choice of an implicit scheme. The final incremental value of the rotation is independent of the initial perturbation as long as this first guess remains within the range of convergence of the iterative scheme.

Finally, a comparison with the rate-independent solution is found useful for explaining a second stage in the development of the instability. An expression for the P–θ relation in the initial post-buckling regime of the rate-independent Shanley column can be found in the work of Sewell (1965). This relation is plotted in Fig. 6 for the earliest possible bifurcation load defined by the tangent modulus. This plot shows a continuous increase in load that is fully controlled by the boundary conditions. The rate-dependent response is presented in the same figure for a range of values of viscosity. To retain the full validity of the linear analysis, the system has been perturbed for rate λ of the order of the rate of loading $\bar{v}/L$. For vanishing viscosity, the corresponding critical load thus tends rapidly to the bifurcation load of the rate-independent model. Observe from Fig. 6 that for decreasing viscosity the rate-dependent response converges to the rate-independent solution. Furthermore, the latency between the instant of perturbation and the real development of buckling is found to be greatly reduced as the rate-independent limit is approached. If viscosity effects are only marginal, which is not the case for creep buckling (Rabotnov and Shesterikov, 1957; Hoff, 1958), the predictions of a linear stability analysis can lead to an accurate estimate of the critical load at which buckling become significant. These results are in agreement with the imperfection analysis of Tvergaard (1985) for stiffened plates. Another consequence of the analogous post-buckling response of the rate-independent and

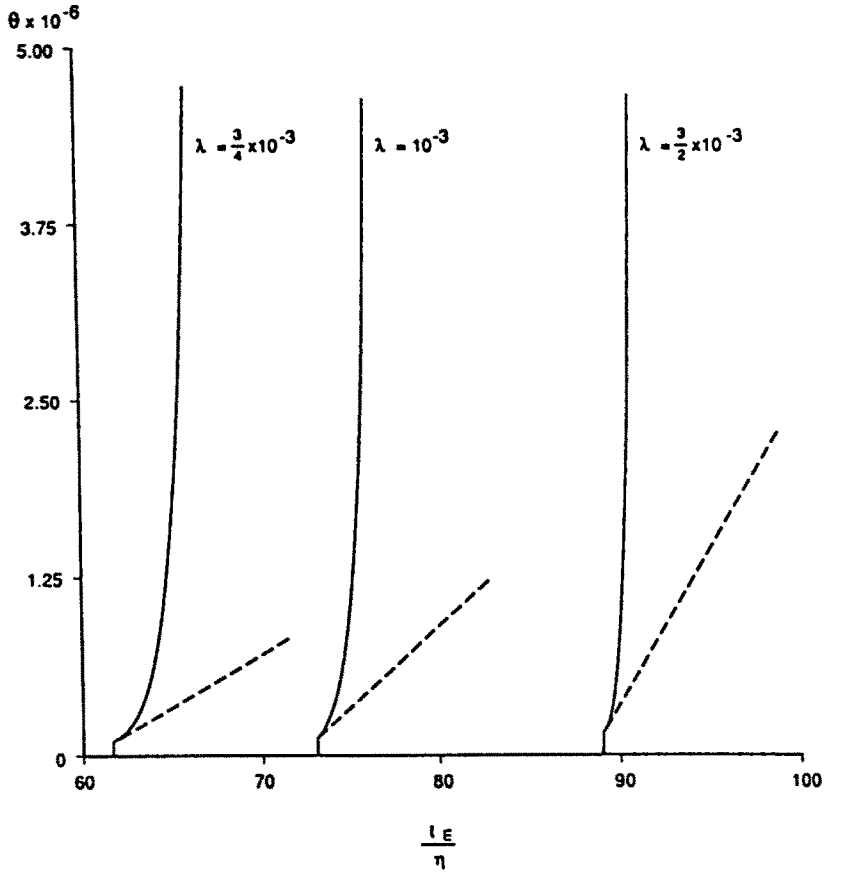

Fig. 5. Close-up of the initial evolution of the angle θ after perturbation of the principal solution, for three different predefined rates of growth λ. The dashed lines represent the predictions of the linear perturbation analysis.

rate-dependent columns is that the growth of the perturbation, predicted to be of an exponential type, must remain bounded and finally determined by the boundary conditions in a later stage of the buckling. This behaviour can be observed from Fig. 7, in which the normalized rotation rate is plotted versus a dimensionless time. Loss of stability of the principal solution of the Shanley column does not lead directly to catastrophic failure of the structure.

3. STABILITY ANALYSIS OF RATE-DEPENDENT SOLIDS

In this section, we wish to broaden the concepts used for the stability analysis of a Shanley column and consider an analogous approach to boundary value problems for rate-dependent solids. A particular emphasis is given to systems with a finite number of degrees of freedom obtained by discretization of the continuum.

The questions of existence and uniqueness of the solution of boundary value problems for rate-dependent solids have been dealt with by Mandel (1971). In particular, the class of materials characterized by no instantaneous permanent deformation is found to be equivalent to linear elastic solids for the discussion of existence and uniqueness. Uniqueness is thus guaranteed when the elastic moduli do not decrease, as a result of, for example, accumulated damage, or for stress levels that remain small compared with these moduli. Of interest here is the stability of this otherwise unique solution. Analysis of loss of stability in shear-band or necking modes has been conducted in the past for simple geometries and material responses (Hutchinson and Obrecht, 1977; Clifton, 1978). In contrast, the analysis to be presented here does not require prior knowledge of the instability modes and is aimed

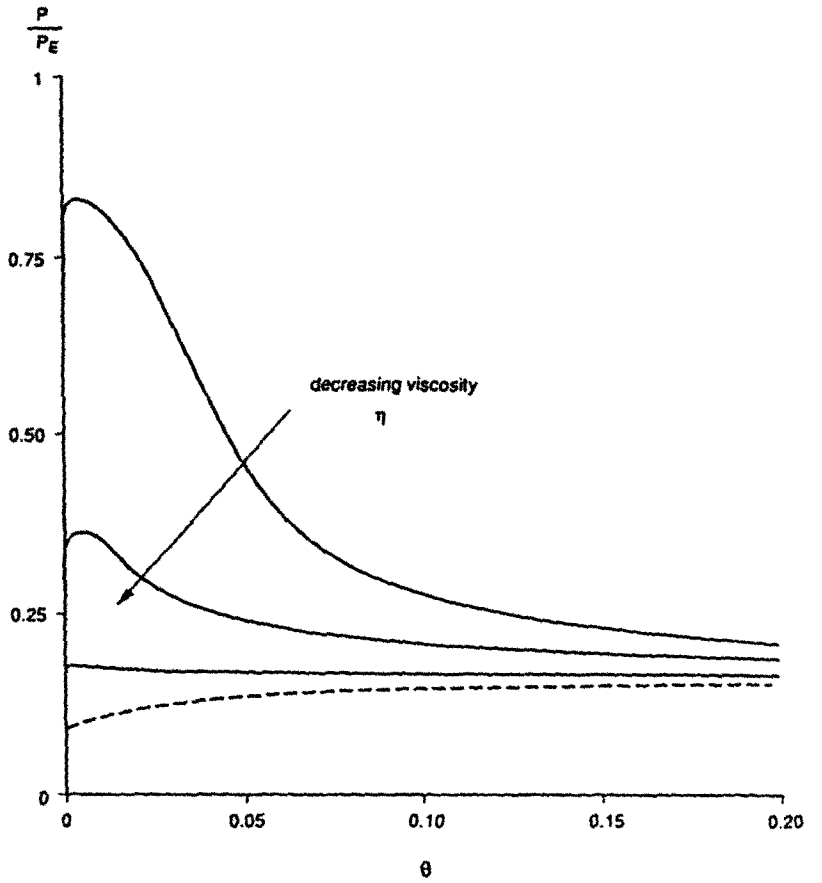

Fig. 6. Load versus rotation of the column, based on the instability threshold. As the viscosity vanishes, the column response tends to the rate-independent solution represented by the dashed curve.

at a general class of material behaviour and an arbitrary domain geometry. To achieve this result, the first step of this section is to introduce a weak formulation of the linear stability criterion. It is then possible to search for the mode of instability and the associated critical load for an equivalent system with a finite number of degrees of freedom, obtained by discretizing the continuum.

Let Ω denote a region with boundary Γ and occupied by a rate-dependent solid. The equations of motion over this domain are:

$$\sigma_{ij,j} + \rho b_i = \rho \ddot{u}_i \quad \text{in} \quad \Omega, \tag{17}$$

where σ_{ij}, ρ, b_i and $\ddot{u}_i$ are respectively the Cauchy stress tensor, the mass density of the material, the body forces vector and the acceleration vector.

We now select a phenomenological constitutive model with no instantaneous permanent deformation, which is appropriate for solids whose main deformation mechanism is dislocation motion (Rice, 1970). More general formulations for elastic–viscoplastic solids can be found in the work of Lubliner (1964) and Mandel (1971). Although a particular choice of formulation has some influence on conditions for uniqueness, it has no bearing on the generality of the stability analysis presented here. The material behaviour considered is described by the following set of equations:

$$\dot{\sigma}_{ij} = D^e_{ijkl}(\dot{\varepsilon}_{kl} - \dot{\gamma} r_{kl})$$

$$r_{kl} = \frac{\partial \psi}{\partial \sigma_{kl}}(\boldsymbol{\sigma}, \mathbf{q})$$

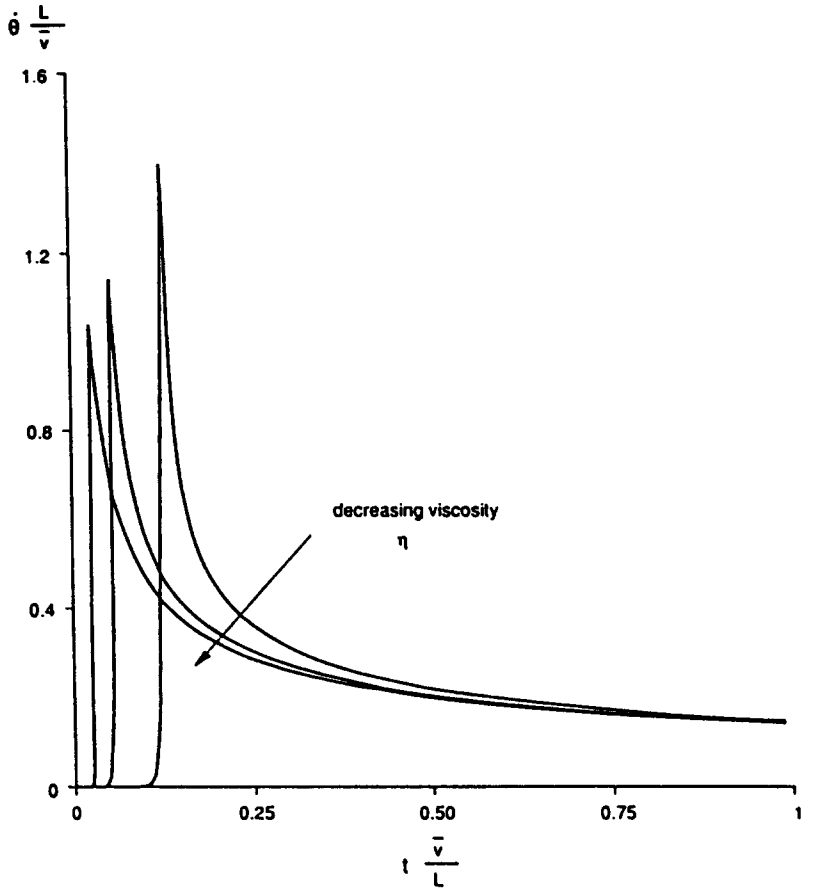

Fig. 7. Evolution of the rotation rate $\dot{\theta}$ with time for various values of the viscosity η. The initial sharp increase remains bounded and the angular evolution is finally controlled by the boundary conditions.

$$\dot{\gamma} = \frac{1}{\eta}\phi(\sigma, \mathbf{q})$$

$$\dot{q}_\alpha = \dot{\gamma} h_\alpha(\sigma, \mathbf{q}), \tag{18}$$

where D^e_{ijkl} are the elastic moduli, $\dot{\varepsilon}_{kl}$ the rates of deformation, r_{kl} the flow directions based on a potential ψ and $\mathbf{q}$ is a family of internal variables. The effective strain rate $\dot{\gamma}$ is defined by a viscosity law $\phi(\sigma, \mathbf{q})$ and the viscosity η. It is assumed here that the function ϕ is zero in some elastic domain defined by σ and $\mathbf{q}$. The fact that the effective plastic strain rate $\dot{\gamma}$ is not a function of any rate quantities but is a function only of the stress tensor σ and the collection of internal variables $\mathbf{q}$, which characterize the current state, is responsible for the instantaneous response being purely elastic. The last equation in (18) represents an evolution equation for the internal variables with the restrictive hypothesis that this evolution is controlled by plastic straining alone.

For simplicity in this presentation, the strain–displacement compatibility equations are written within a small strain approximation:

$$\varepsilon_{ij} = \tfrac{1}{2}(u_{i,j} + u_{j,i}). \tag{19}$$

The absence of non-linear terms in (19) precludes a certain class of instabilities from this analysis but does not affect is generality.

To complete the set-up of the problem, consider the following mixed-boundary conditions:

$$\sigma_{ij}n_j = \bar{t}_i \quad \text{on} \quad \Gamma_t$$
$$u_i = \bar{u}_i \quad \text{on} \quad \Gamma_u$$
$$\text{with} \qquad \Gamma_u \cap \Gamma_t = \varnothing \quad \text{and} \quad \Gamma_u \cup \Gamma_t = \Gamma. \tag{20}$$

The solution of the governing equations and boundary conditions (17)–(20) is called the principal solution of the problem and is denoted by the superscript $(\,)^0$. As already mentioned, constant moduli D^e_{ijkl} guarantee uniqueness of the solution for stress levels that remain small compared with these moduli and bifurcation is thus precluded. We now study the stability of this principal solution and consider perturbed solutions of the following type at time $\tau = t + \Delta t$ for Δt small compared with unity:

$$A(\mathbf{x}, \tau) = A^0(\mathbf{x}, \tau) + \varepsilon \delta A(\mathbf{x}, \tau) \quad \text{with} \quad \varepsilon \ll 1. \tag{21}$$

The function $A(\mathbf{x}, \tau)$ is generic for all field quantities and δA denotes a perturbation added to the principal mode $A^0(\mathbf{x}, \tau)$. Unlike the discrete case of the Shanley column, the perturbations now have spatial variations which are additional unknowns in this problem. Such perturbations are admissible at time τ if they satisfy the appropriate field equations and boundary conditions. Considering the admissibility of solutions of type (21), we obtain as in the first section two problems of different order, the zero-order problem characterizing the principal solution at time τ. The first-order problem takes the form:

$$\delta\sigma_{ij,j} = \rho\delta\ddot{u}_i \quad \text{in} \quad \Omega, \quad \delta\sigma_{ij}n_j = 0 \quad \text{on} \quad \Gamma_t$$
$$\delta u_i = 0 \quad \text{on} \quad \Gamma_u$$
$$\delta\dot{\varepsilon}_{ij} = \tfrac{1}{2}(\delta\dot{u}_{i,j} + \delta\dot{u}_{j,i})$$
$$\delta\dot{\sigma}_{ij} = D^e_{ijkl}\left[\delta\dot{\varepsilon}_{kl} - \delta\dot{\gamma}r^0_{kl} - \dot{\gamma}^0\left(\frac{\partial r_{kl}}{\partial \rho_{mn}}\bigg|^0 \delta\sigma_{mn} + \frac{\partial r_{kl}}{\partial q_\alpha}\bigg|^0 \delta q_\alpha\right)\right]$$
$$\eta\delta\dot{\gamma} = \frac{\partial \phi}{\partial \sigma_{ij}}\bigg|^0 \delta\sigma_{ij} + \frac{\partial \phi}{\partial q_\alpha}\bigg|^0 \delta q_\alpha$$
$$\delta\dot{q}_\alpha = \dot{\gamma}^0\left(\frac{\partial h_\alpha}{\partial \sigma_{ij}}\bigg|^0 \delta\sigma_{ij} + \frac{\partial h_\alpha}{\partial q_\beta}\bigg|^0 \delta q_\beta\right) + \delta\dot{\gamma}h^0_\alpha. \tag{22}$$

Focussing on the initial behaviour of the perturbations, we now choose to study the solution of (22) of the form:

$$\delta A(\mathbf{x}, \tau) = \delta\hat{A}(\mathbf{x}) \exp(\lambda \Delta t), \tag{23}$$

where again λ is the initial rate of growth of the perturbations. Solution of (22) with the proposed structure (23) requires the evolution of the perturbation to be rapid compared with the variation of the coefficients of the first-order problem, so that they can be considered nearly constant over some interval of time. If solutions of (22) are found for positive rate λ, then the perturbation can initially grow, otherwise stability is ensured. A loss of stability indicates that the principal solution that remains the solution of a well-posed problem is not physically observable. The limiting process of Δt tending to zero is now considered and the first-order problem (22) for solutions of type (23) is rewritten as:

$$\delta\dot{\sigma}_{ij,j} = \rho\lambda^2\delta\hat{u}_i \quad \text{in} \quad \Omega, \quad \delta\dot{\sigma}_{ij}n_j = 0 \quad \text{on} \quad \Gamma_t$$

$$\delta\hat{u}_i = 0 \quad \text{on} \quad \Gamma_u$$

$$\delta\hat{\varepsilon}_{ij} = \tfrac{1}{2}(\delta\hat{u}_{i,j} + \delta\hat{u}_{j,i})$$

$$\delta\dot{\sigma}_{ij} = D^e_{ijkl}\left[\delta\hat{\varepsilon}_{kl} - \delta\hat{\gamma}r^0_{kl} - \frac{\dot{\gamma}^0}{\lambda}\left(\frac{\partial r_{kl}}{\partial\sigma_{mn}}\bigg|^0 \delta\dot{\sigma}_{mn} + \frac{\partial r_{kl}}{\partial q_\alpha}\bigg|^0 \delta\hat{q}_\alpha\right)\right]$$

$$\eta\delta\hat{\gamma} = \frac{1}{\lambda}\left(\frac{\partial\phi}{\partial\sigma_{ij}}\bigg|^0 \delta\dot{\sigma}_{ij} + \frac{\partial\phi}{\partial q_\alpha}\bigg|^0 \delta\hat{q}_\alpha\right)$$

$$\delta\hat{q}_\alpha = \frac{\dot{\gamma}^0}{\lambda}\left(\frac{\partial h_\alpha}{\partial\sigma_{ij}}\bigg|^0 \delta\dot{\sigma}_{ij} + \frac{\partial h_\alpha}{\partial q_\beta}\bigg|^0 \delta\hat{q}_\beta\right) + \delta\hat{\gamma}h^0_\alpha. \tag{24}$$

Further reduction of eqns (24d)–(24f), corresponding to the first-order problem of the constitutive equations, yields a relation of the type:

$$\delta\dot{\sigma}_{ij} = D_{ijkl}(\lambda)\,\delta\dot{\varepsilon}_{kl}, \tag{25}$$

for some moduli $D_{ijkl}(\lambda)$ that are functions of λ. Note that a tractable expression for the moduli D_{ijkl} is obtainable for simple functions ψ and ϕ, but the resulting general expression is not appropriate for further analytic development. Nevertheless, it is possible to analyse the structure of relation (25) by simply examining eqns (24d)–(24f). Two limiting cases are considered, as for the Shanley column analysis. Consider first the case of infinite rate of growth λ. Owing to the presence of the term in $1/\lambda$, the contribution from the plasticity part of the constitutive equations vanishes and the moduli $D_{ijkl}(\lambda \to \infty)$ are nothing but the elastic moduli. Now consider the other limiting case of vanishing rate of growth ($\lambda \to 0^+$), which corresponds to the first possible instability. To remain within the domain of validity of this analysis, one needs to consider at the same time vanishing slow process $\dot{\gamma}_0$. From (18c), it is clear that this limit is equivalent to the replacement of the viscosity law by a yield criterion $\phi(\sigma, \mathbf{q}) = 0$. The moduli $D_{ijkl}(\lambda \to 0^+)$ are thus obtained by considering a rate-independent model that is obtained as the limit of inviscid flow of the rate-dependent one. A similar conclusion was already reached in the rather different problem of shear-band initiation in single crystals by Molinari (1988).

An important consequence of the presence of viscosity effects is that it eliminates questions concerning the choice of loading or unloading conditions encountered in bifurcation analyses for rate-independent plasticity models. In the part of the domain Ω where plastic flow is taking place ($\phi > 0$), no instantaneous unloading is possible even for vanishing viscosity. In such a region and for the earliest instability defined by a vanishing rate λ, the moduli $D_{ijkl}(\lambda \to 0^+)$ are obtained from the rate-independent model pertaining as the limit of inviscid plastic flow is approach. The analysis for the earliest instability thus yields Hill's linear comparison solid (Hill, 1958). Consequently, for plasticity models with an associated flow rule, the instability threshold does indeed correspond to the first bifurcation of the corresponding rate-independent model.

The next step in a classical linear stability analysis is to assume some specific modes of perturbation $\delta\hat{A}$, guided by the physics of the problem. Instead of postulating these functions we retain them as unknowns and rely on numerical methods to obtain solutions for systems with a finite number of degrees of freedom. Accordingly, we now consider the following weak form of the first-order problem:

$$\int_\Omega [\delta\dot{\sigma}_{ij,j}(\mathbf{x}, t) - \rho\lambda^2\delta\hat{u}_i(\mathbf{x})]\eta_i\,\mathrm{d}\Omega - \int_{\Gamma_t} \delta\dot{\sigma}_{ij}n_j\eta_i\,\mathrm{d}\Gamma = 0, \tag{26}$$

for some test functions η_i that satisfy the essential boundary conditions (22b). An integration by parts and use of the constitutive relation (25) and compatibility eqn (24c) yields:

$$\int_\Omega \eta_{i,j} D_{ijkl}(\lambda)\delta\hat{u}_{k,l}\,d\Omega + \lambda^2 \int_\Omega \rho\eta_i\delta\hat{u}_i\,d\Omega = 0. \tag{27}$$

Considering, for example, a finite-element formulation with the same interpolation for the test functions and for the displacements, we obtain a discretized version of the first-order problem, which in matrix notation reads:

$$\left[\sum_e \int_{\Omega_h^e} \mathbf{B}^T\mathbf{D}(\lambda)\mathbf{B}\,d\Omega_h^e + \lambda^2 \int_{\Omega_h^e} \rho\mathbf{N}^T\mathbf{N}\,d\Omega_h^e\right]\delta\hat{\mathbf{u}}_h = 0. \tag{28}$$

The summation extends over all elements and the strain operator **B** is based on the shape functions present in **N**. For the nodal displacement perturbation $\delta\hat{\mathbf{u}}_h$ to have a non-trivial solution, the condition:

$$\det(\mathbf{K}(\lambda) + \lambda^2\mathbf{M}) = 0 \tag{29}$$

must hold. Here **K** is a stiffness array based on the moduli $\mathbf{D}(\lambda)$ and **M** is the mass array.

The linear stability analysis of the boundary value problem (17)–(20) has thus been expressed as an eigenvalue analysis over a discretized domain. A zero eigenvalue in (29) corresponds to a loss of stability of the solution and the corresponding eigenvector $\delta\hat{\mathbf{u}}_h$ is the instability mode in terms of the displacement field of the discretized system. Two potential applications of this stability analysis can be foreseen. It can first be used at a final stage in a stability analysis to obtain approximate solutions in the absence of any analytic results. Secondly, owing to the simple formulation of the criterion (28), it can be incorporated as a standard option in finite-element programs to check the stability of the computed solution.

4. APPLICATION TO THE PLANE STRAIN TENSION TEST

As an application of the previous section, we now study the stability of a rectangular specimen consisting of a von Mises solid. The specimen is sustaining an homogeneous plane strain deformation under tensile loading, which is called the fundamental mode of deformation in this problem. It is known from experimental works (e.g. Anand and Spitzig, 1980), from the bifurcation analysis of Hill and Hutchinson (1975) and from the numerical simulations of Tvergaard *et al.* (1981) that the deformation could depart from the initial homogeneous mode at some point of the loading. This deviation initiates the localization of the deformation in shear bands, which is the failure mode of the specimen. The goal of this numerical analysis is to detect the onset and to follow the development of this localization process for the case of a rate-dependent solid.

A particular model is now selected from the general class of materials introduced in (18). Its elastic response is chosen to be linear with a Young's modulus and Poisson's ratio of 10^3 MPa and 0.3, respectively. The plastic flow potential ψ in (18b) is the von Mises effective stress σ_e and the viscosity law (18c) is of a power-law type:

$$\dot{\gamma} = \dot{\gamma}_0\left[\left(\frac{\sigma_e}{\sigma_0(\gamma)}\right)^m - 1\right] \quad \text{for} \quad \sigma_e \geqslant \sigma_0(\gamma), \quad \text{zero otherwise.} \tag{30}$$

In this relation, σ_0 is a reference stress function of the effective plastic strain γ, and $\dot{\gamma}_0$ a constant reference strain rate, set to $10^{-3}\ s^{-1}$ in the whole analysis. The rate sensitivity is controlled by the strain-rate exponent m with the limit of inviscid flow obtained for infinitely large values of this exponent. The hardening function $\sigma_0(\gamma)$ is expressed as the product of a power law and an exponential function:

$$\sigma_0(\gamma) = (\sigma_y - \sigma_c)\left(1+\frac{\gamma}{\gamma_1}\right)^n \exp\left(-\frac{\gamma}{\gamma_2}\right)+\sigma_c. \tag{31}$$

The exponential function in (31) models in a simple way the degradation of the flow stress as plastic deformation accumulates. It is the key factor that renders possible the localization of the deformation in shear bands in this problem. The introduction of σ_c ensures the existence of a non-vanishing strength in the fully hardened state. Values of 10^{-3} and 5×10^{-3} are chosen for the two reference strains γ_1 and γ_2 and the hardening exponent n is set to 3/4. The initial reference yield stress σ_y and the cut-off stress σ_c have values of 1 and 0.1 MPa, respectively. The material response is shown in Fig. 8 for two different values of the strain rate exponent m and for a nominal strain rate of $4/3 \times 10^{-3}\ s^{-1}$.

The domain, which is first discretized with 10×15 four-node quadrilaterals, comprises a quarter of the specimen for reasons of symmetry. As a consequence, we focus our attention on instability modes that have the same geometrical properties. A discussion of the role of asymmetric modes in the localization process can be found in the work of de Borst (1988, 1989). Despite the homogeneous character of the principal solution, a treatment of the plasticity incompressibility constraints based on the $\bar{\mathbf{B}}$ method (Hughes, 1980) is adopted. This procedure eliminates the overly stiff response of the element when extensive plastic flow occurs and is a prerequisite to capture the spacial gradient of the modes of instability. Nevertheless, it should be noted that such treatment does not improve the poor performance of isoparametric elements in localization analysis, as shown by Ortiz *et al.* (1987). Owing to a continuous strain interpolation, isoparametric elements have been identified as inhibiting the growth of shear bands, unless the band orientations coincide with the elements'

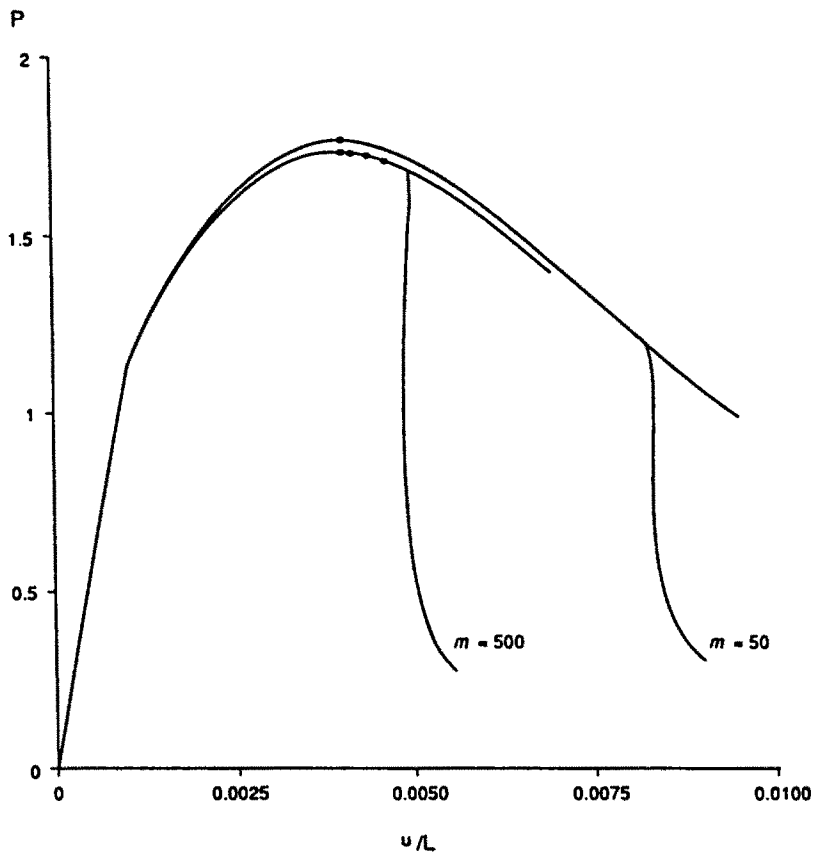

Fig. 8. Comparison of load–displacement curves between the perturbed solutions and the fundamental one. Two values of the rate exponent m are considered.

boundaries. Careful mesh design is thus required to minimize the numerical band broadening that could otherwise mask effects of the real physical mechanism responsible for localization. An example of such a mesh design can be found in the work of Tvergaard *et al.* (1981), and Tvergaard (1982), for crossed-triangle quadrilateral elements. A review of finite-element methods for localization analysis is presented by Leroy *et al.* (1989). In this paper, to improve the performance of the four-node quadrilateral, we choose a finite-element scheme introduced by Ortiz *et al.* (1987). In their scheme, the conventional strain interpolation is complemented by specialized modes of deformation that fully accommodate shear banding at the local level. The resulting enhanced element was observed to reduce the mesh sensitivity to the development of arbitrary oriented shear bands successfully, in both two- and three-dimensional problems (Leroy and Ortiz, 1989, 1990). A generalization to the finite deformation context was proposed by Nacar *et al.* (1990). The formulation for transient problems of this new finite-element method presented by Leroy and Ortiz (1990) is adopted in this paper.

To complete the description of this numerical analysis, note that the displacement of the top of the specimen is prescribed as a function of time. This function is initially linear and thus corresponds to a constant nominal strain rate. As the localization of the deformation takes place, the strain rate could increase drastically in the shear bands. To control such an evolution, it is chosen to modify the loading function such that the strain rate at any point of the mesh be at most the initial nominal strain rate. The resulting mixed finite-element method has been used in various contexts by Riks (1979), Tvergaard *et al.* (1981) and de Borst (1987), and is close to the one proposed by Chen and Schreyer (1990).

During the homogeneous straining of the specimen, two modes of instability are expected, necking modes and shear bands. We now review results from the literature concerning the initiation and the growth of such modes of instability in rate-dependent solids. This information is essential to enable the validity of the numerical stability analysis presented in this section to be assessed. The necking type of instability in infinite bars creeping according to a power law has been investigated by several authors. Hutchinson and Obrecht (1977) have shown that under quasi-static conditions, while perturbations of all wavelengths are admissible, the modes with long wavelength had the fastest growth. Hutchinson and Neale (1977) further pointed out the strong retarding effect on the development of localization of even a low viscosity. The conclusions are different under dynamic conditions. Inertia has a stabilizing effect on the growth of long-wavelength modes and multiaxial effects have the same influence on the shorter ones and result in an intermediate critical wavelength (Fressengeas and Molinari, 1990). In this study, the specimen is of a given aspect ratio and only discrete values of the continuous spectrum of wavelength are admissible. Furthermore, because of the material hardening and by analogy to the rate-independent case (Hill and Hutchinson, 1975), the long-wavelength mode is expected to be the first admissible wave mode. The second type of instability to be expected is shear bands. The only kinematic constraint for their development is that their orientation must be compatible with the aspect ratio of the specimen. Here, by choosing an aspect ratio of 3/2, shear bands are kinematically admissible modes of instability. Localization of the deformation into shear bands is known to be delayed by rate effects (Molinari and Clifton, 1987). Under dynamic conditions, inertia has a further stabilizing effect, while heat generation has the opposite effect and accelerates the localization process (Molinari and Clifton, 1987).

The results concerning the linear stability analysis of the fundamental solution are now presented. Attention is focussed here on perturbations having initially a vanishing rate of growth and thus corresponding to the first instability. The strain rate exponent m is set to 500, rendering the material only slightly rate-sensitive. The particular choice of plasticity flow rule and viscosity law in this example results in a tangent operator in (25) having major symmetry. The stiffness matrix $\mathbf{K}(\lambda)$ in (28) is thus symmetric and is initially positive definite. The lowest eigenvalue of the system (28) is obtained by the inverse iteration method (Wilkinson, 1965). The vanishing of the lowest eigenvalue signals the onset of an unstable solution. The first four modes of instability are shown in Figs 9a–9d. These figures present the normalized displacement eigenvectors of system (28) associated with the first four zero eigenvalues. The finite-element solutions to the instability modes are all of a wave type.

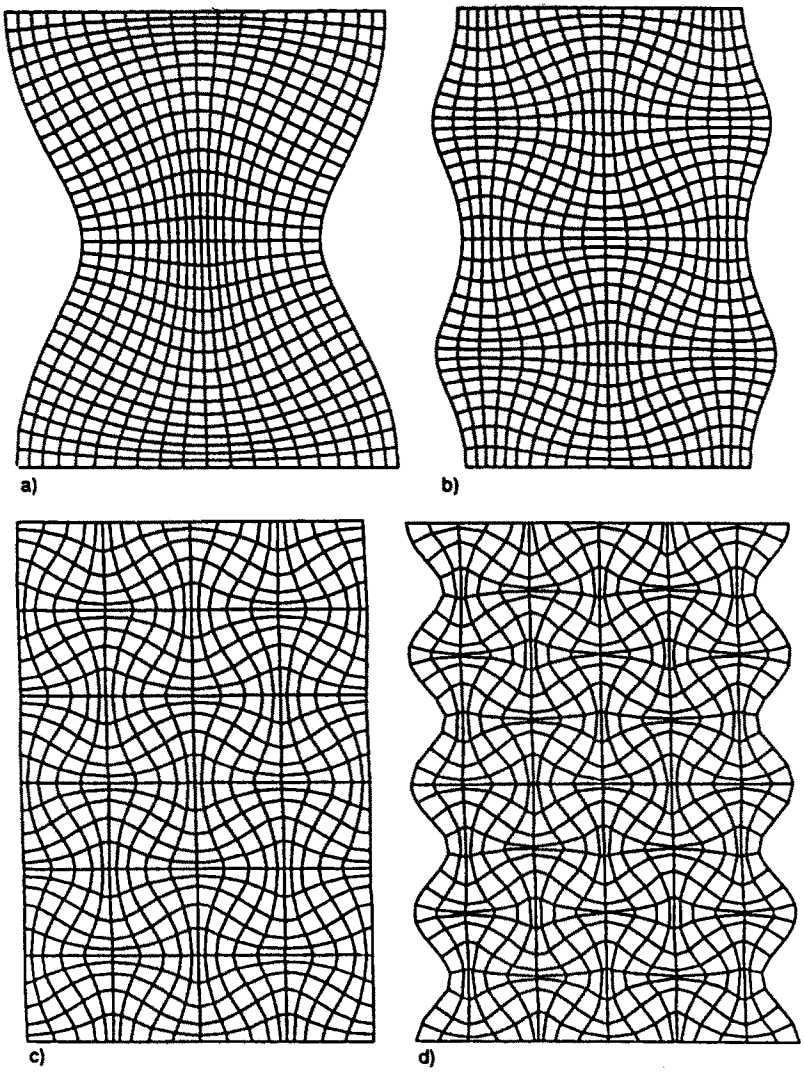

Fig. 9. The first four instability eigenmodes in terms of the displacement field, for a von Mises solid under plane strain tension.

Following the chronological order of occurrence of these modes from Figs 9a–9d, one observes the wavelength to decrease in both spatial directions. The loads at which these instabilities are detected are marked by points on the load–displacement curve of Fig. 8. Note that the first instability is detected just beyond maximum load, an expected result since we are considering perturbations with vanishing initial rate of growth and thus corresponding to a limit to a rate-independent response. In concluding this linear stability analysis, we comment on the absence of shear bands as initial instability modes. These modes, as already stated, are kinematically admissible. Furthermore, the local criterion for shear band initiation used by Leroy and Ortiz (1990) is found to be satisfied at every point of the mesh at the critical time when the first mode of instability is detected. This discrepancy could be due to the absence of a preferential site for the initiation of shear bands, and hence they remain latent. This interpretation is confirmed by the analysis of de Borst (1989), who observe shear-band mode of instabilities in a rate-independent solid only when imperfections were introduced.

From the preceding linear stability analysis, we consider the principal solution to be unstable as soon as a zero eigenvalue is detected. Nevertheless, as for the discrete case of the Shanley column, monitoring the evolution of the perturbed solution is required in order to assess whether the principal mode of deformation is asymptotically unstable.

The evolution of the principal solution perturbed with the first eigenmode, Fig. 9a, is now studied. This perturbation of the fundamental solution is achieved by prescribing the first iteration of the next incremental displacement field to be a small fraction of the eigenmode (order of magnitude 10^{-5}). The corresponding load–displacement curve is presented in Fig. 8. After a latency, a sudden drop in the bearing capacity of the specimen is recorded. This change in the structural response is associated with the development of a shear band oriented at about 45° to the horizontal axis. The thickness of this band rapidly decreases and attains the minimum width set by the mesh. Furthermore, note that the load–displacement curve in Fig. 8 exhibits a snap-back. It was necessary to reverse momentarily the displacement at the boundary to stabilize the development of the localization process. This result indicates that when specialized elements are used, hence in the absence of any numerical stiffnesses, the viscosity of the constitutive model is not sufficient to stabilize the catastrophic localization phenomenon. This shear-band failure mode can be defined as a continuous increase in strain rate in a band of decreasing thickness. This observation also indicates that localization should be interpreted as a dynamic process even in a kinematically controlled experimental set-up. The deformed mesh where the displacement field is magnified is presented in Fig. 10. Figure 11 shows the normals of the two directions along which shear bands could develop in every element in which plastic flow is still taking place at the end of the test. This information is used at the local level to define the extra modes of deformation introduced in the finite-element method (Ortiz *et al.*, 1987; Leroy and Ortiz, 1990). These two figures show a variation in shear-band thickness of two elements to one element from the specimen centre to its free boundary. The ability of the finite-element method to accommodate localization up to the smallest mesh size can be judged from these results.

The influence of the strain rate exponent m, controlling the rate sensitivity of the solid, is assessed by repeating the same analysis for a higher value of $m = 50$, corresponding to a more viscous response. The load–displacement curve for the principal solution of this problem can be found in Fig. 8. On this curve, the point marks the first possible occurrence of an instability that turns out to be a long wavelength mode analogous to the one presented in Fig. 9a. After the perturbation of the system, the solution reveals the development of shear bands, which dominate the necking mode as in the previous test; see Figs 12 and 13. This time, the latency before initiation of localization is increased, whereas the snap-back

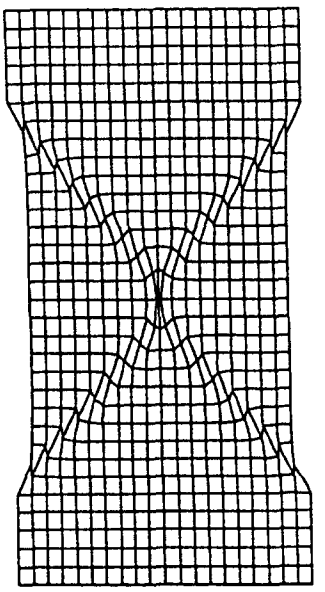

Fig. 10. Deformed mesh showing a double shear band. Displacement field magnified by 30, rate exponent m of 500.

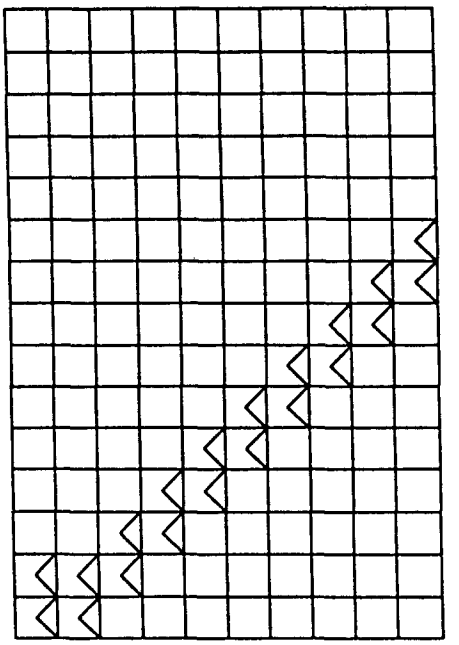

Fig. 11. The normals to the shear-band directions are represented in each element in which plastic flow is still taking place at the end of the test. Only the upper quarter of the specimen is presented. Rate exponent m of 500.

in the load–displacement curve is only marginal. This illustrates the strong retarding effect of viscosity on the growth of the localized deformation.

To estimate the sensitivity of the simulated localization process to the mesh size, the same problem is repeated for a finer mesh of 20×30 elements and for $m = 50$. The results are given in Figs 14 and 15. The initial mode of perturbation $\delta\hat{\mathbf{u}}_k$ and the stability threshold converge towards the continuum solution, as the mesh size is decreased. This improved resolution has some bearing on the exact final distribution of the shear bands, which are

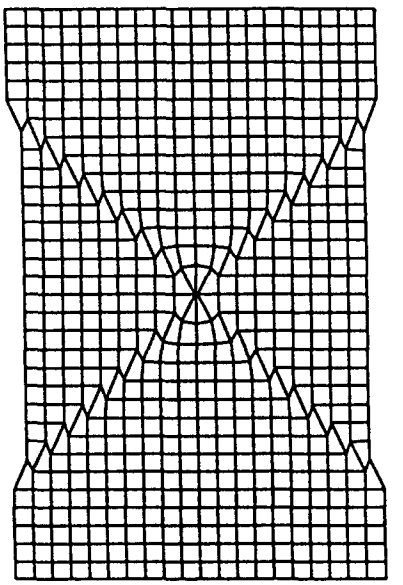

Fig. 12. Deformed mesh showing a double shear band. Displacement field magnified by 25, rate exponent m of 50.

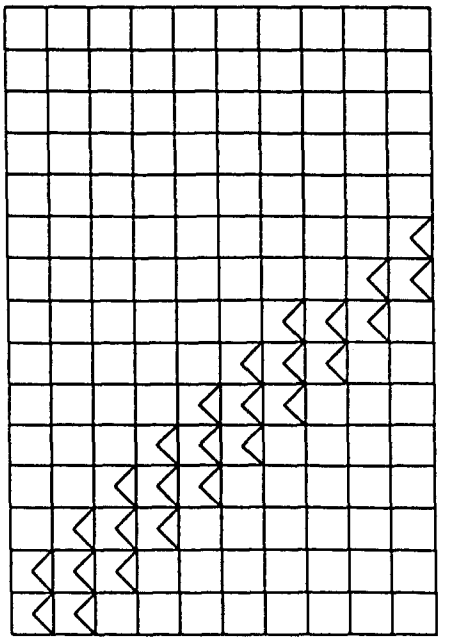

Fig. 13. The normals to the shear band directions are represented in each element in which plastic flow is still taking place at the end of the test. Only the upper quarter of the specimen is presented. Rate exponent m of 50.

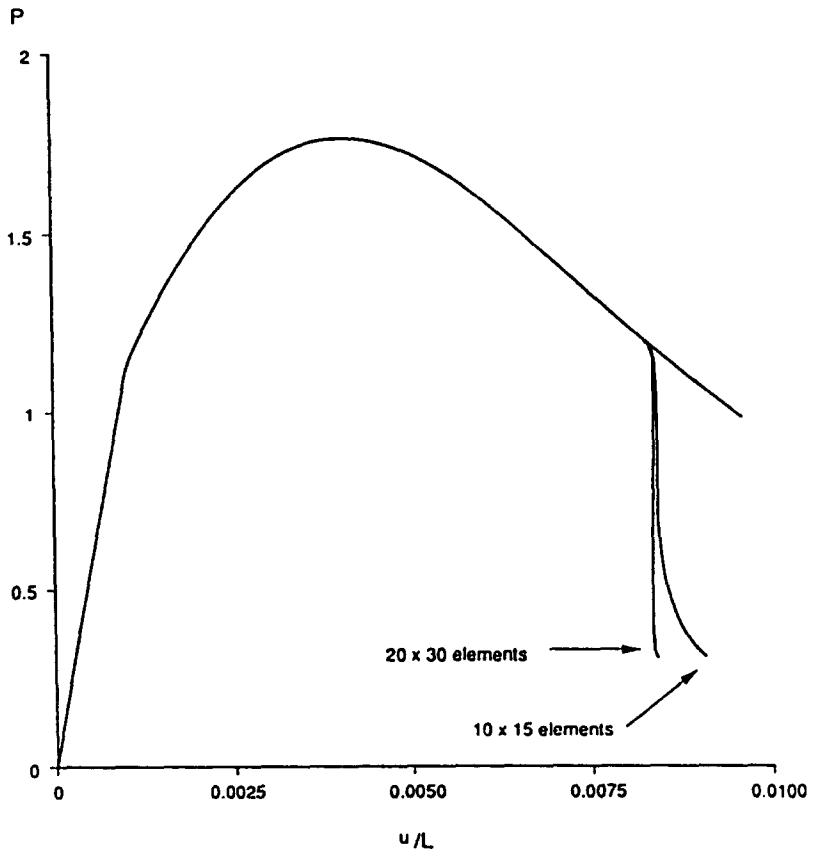

Fig. 14. Comparison of load–displacement curves between the perturbed solution and the fundamental one, for two meshes of 10 × 15 elements and 20 × 30 elements. Rate exponent m of 50.

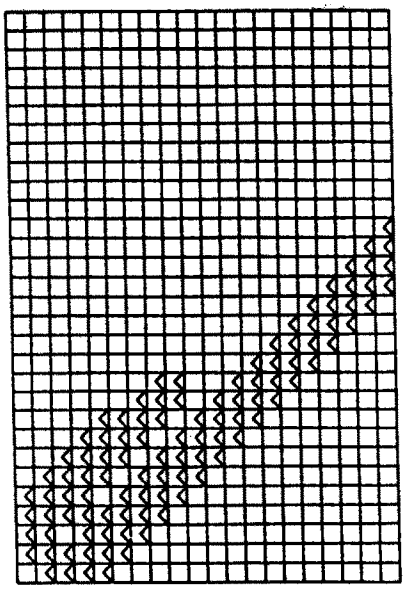

Fig. 15. Distribution of the plastic zone and orientation of the shear band at an intermediate stage of the test for a mesh of 20 × 30 elements. Rate exponent m of 50. Perturbation based on the first mode of Fig. 9.

now observed to be deviated from the specimen centre and to be reflected on the symmetry boundaries. During the localization process, two parallel bands are first observed in each quarter of the specimen. In time, the upper band is found to unload while shear localization continues in the lower one. This process can be observed in Fig. 15, at an intermediate stage of the localization process. At a later stage, the upper band has completely unloaded, leaving only some traces in the deformation.

A final question dealt with here concerns the influence of the wavelength of the perturbation on the final failure mode of the specimen. Once the principal solution is perturbed by a long-wavelength mode, criterion (28) can still be used to assess the stability of the new solution. A shorter-wavelength mode, analogous to the one presented in Fig. 9b, becomes rapidly available. Hence it was decided to conduct a second perturbation to study the influence of this shorter wave mode. This analysis is considered for the finer mesh size and a rate exponent of $m = 50$. The results are presented in Figs 16 and 17. Despite the presence of the shorter wave mode, the long wave mode is observed to have the fastest growth, thus resulting in the development of a single set of shear bands. This result is in agreement with the analysis of Hutchinson and Obrecht (1977). The only difference between this test and the previous single perturbation test is the position of the bands on the specimen, which are this time found to cross the centre; see Fig. 17. The same influence of shorter wave modes on the final location of the shear bands was also observed by Tvergaard *et al.* (1981). In their work, the two perturbations were initially introduced as geometric defects with different wavelength.

Compare now the band thickness at the end of the tests for $m = 50$ and for the two different mesh sizes; see Figs 17 and 13. It is apparent that the simulated bands always have a thickness varying from two or three elements to a minimum of one element, regardless of the mesh size. This seems to indicate that the physical problem of shear banding in rate-dependent solids is one with no stationary solutions, and that the numerical solutions are valid up to a time when the narrowing band has attained the minimum thickness defined by the mesh.

5. CONCLUSION

The introduction of deformation-rate sensitivity ensures the existence of a unique solution to boundary value problems when characteristic stress levels remain small compared with the elastic moduli (Mandel, 1971). Rate sensitivity is proposed to explain the

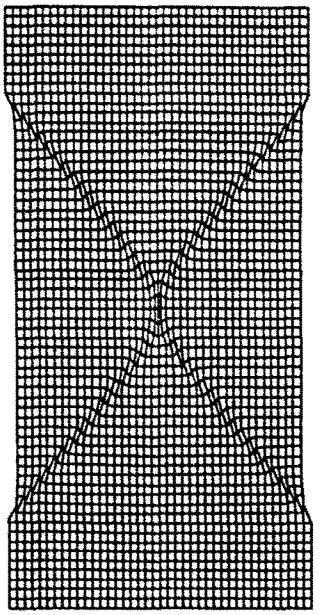

Fig. 16. Deformed mesh showing a single shear band for a mesh of 20 × 30 elements. Displacement field magnified by 40, rate exponent m of 50. Two perturbations are considered, corresponding to the two first eigenmodes of Fig. 9.

behaviour of materials such as metals under high strain rates (Marchand and Duffy, 1988). By considering the limit of inviscid flow in a rate-dependent model, a rate-independent behaviour is obtained that is also appropriate to describe a large class of materials such as rocks and granular materials, under a variety of loading conditions. Nevertheless, this limiting process does not suppress the essential feature of the rate-dependent formulation, which is to guarantee the well-posedness of the problem, paramount in any localization analysis.

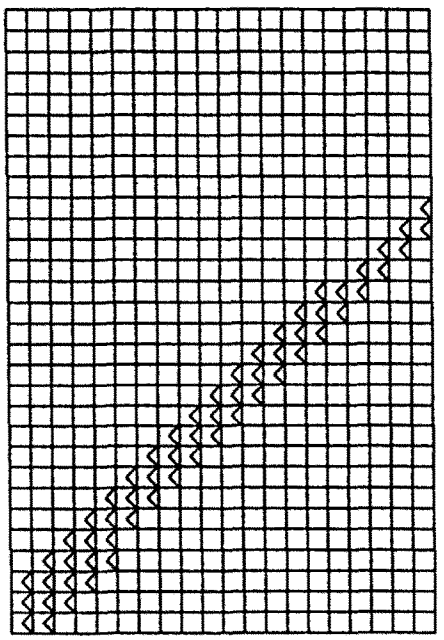

Fig. 17. Distribution of the plasticity domain and orientation of the shear band at the end of the test with a rate exponent m of 50 and a mesh of 20 × 30 elements. Perturbations correspond to the two first eigenmodes of Fig. 9. Only the upper quarter of the specimen is presented.

Uniqueness in the solution of a given boundary value problem does not imply its stability under small perturbations. Whereas a solution regardless of its stability can be analysed either analytically or by choosing the appropriate numerical scheme, its physical existence is conditional to its stability. This concept was first illustrated here in the case of the Shanley column. A loss of uniqueness in the principal solution of an untilted column occurs at the Euler load under quasi-static conditions and the stability threshold is found to coincide with a critical load defined by the tangent modulus obtained as the limit of inviscid plasticity is approached. For every load beyond this threshold a potential perturbation corresponds with a positive rate of growth, which leads to the buckling of the column. The latency between the instability threshold and the real occurrence of buckling is found to vanish for decreasing viscosity. Unlike the results of creep buckling analyses (Rabotnov and Shesterikov, 1957; Hoff, 1958), linear stability predictions can thus be very representative of the actual buckling load of a structure, as the limit of inviscid plastic flow is approached.

For solids under multiaxial conditions, a similar linear stability analysis of the Shanley column discrete case can be considered, and a weak formulation of the stability criterion has been presented. For systems with finite degrees of freedom typically obtained by discretization of the continuum, a numerical solution can be obtained to both the instability threshold and the corresponding eigenmode. It is necessary to monitor the evolution of the perturbed solution to confirm the prediction of the linear stability analysis. Furthermore, this exercise can reveal the development of localization phenomena which are usually responsible for the final failure. This concept has been applied here to the finite-element simulation of a von Mises rectangular block under plane strain tensile loading. Whereas the initial modes of instability were found to be of a wavy type, the final failure mechanism was in shear banding. The influence of both the rate sensitivity and the wavelength of the mode of perturbation on the development of shear bands has been considered. The presence of rate effects delayed the development of shear bands but could not stabilize the catastrophic localization phenomenon. The introduction of short-wavelength perturbations affected the final position of the shear bands on the specimen. Finally, a convergence analysis confirmed the dependence of the simulated band thickness on the smallest mesh size and seems to indicate the non-existence of a stationary solution for the class of rate-dependent solids considered here.

Acknowledgements—The author wishes to extend his sincere appreciation to Professor A. Molinari (Université de Metz, France) for his continuous interest and encouragement during the course of this work. Helpful discussions with F. K. Lehner (Koninklijke/Shell Exploratie en Produktie Laboratorium) and Professor N. Triantafyllidis (University of Michigan) during the preparation of this manuscript are also gratefully acknowledged. This paper is published by the kind permission of Shell Internationale Research Maatschappij.

REFERENCES

Anand, L., Kim, K. H. and Shawki, T. G. (1987). Onset of shear localization is viscoplastic solids. *J. Mech. Phys. Solids* **35**, 407–429.

Anand, L. and Spitzig, W. A. (1980). Initiation of localized shear bands in plane strain. *J. Mech. Phys. Solids* **28**, 113–128.

Arnold, V. I. (1973). *Ordinary Differential Equations*. The MIT Press, Cambridge, MA.

Bai, Y. L. (1982). Thermo-plastic instability in simple shear. *J. Mech. Phys. Solids* **30**, 195–207.

de Borst, R. (1987). Computation of post-bifurcation and post-failure behavior of strain-softening solids. *Comput. Struct.* **25**, 211–224.

de Borst, R. (1988). Bifurcations in finite element models with a non-associated flow law. *Int. J. Numer. Anal. Meth. Geomech.* **12**, 99–116.

de Borst, R. (1989). Numerical methods for bifurcation analysis in geomechanics. *Ing.-Arch.* **59**, 160–174.

Chen, Z. and Schreyer, H. L. (1990). A numerical solution scheme for softening problems involving total strain control. Preprint.

Clifton, R. J. (1978). Adiabatic shear band. In Report NMAB-356 of the NRC Committee on material response to ultrasonic loading rates.

Coddington, E. A. and Levinson, N. (1955). *Theory of Ordinary Differential Equations*. McGraw-Hill, Scarborough, CA.

Fressengeas, C. and Molinari, A. (1990). Fragmentation of rapidly stretching jets. To be published.

Hadamard, J. J. (1903). *Leçons sur la Propagation des Ondes et les Equations de l'Hydrodynamique*. Hermann, Paris.

Hill, R. (1958). A general theory of uniqueness and stability in elastic-plastic solids. *J. Mech. Phys. Solids* **6**, 236–249.
Hill, R. and Hutchinson, J. W. (1975). Bifurcation phenomena in the plane tension test. *J. Mech. Phys. Solids* **23**, 239–264.
Hoff, N. J. (1958). A survey of the theories of creep buckling. *Proc. Third U.S. National Congress of Applied Mechanics*, ASME, New York.
Hughes, T. J. R. (1980). Generalization of selective integration procedures to anisotropic and nonlinear media. *Int. J. Num. Meth. Engng* **15**, 1413–1418.
Hutchinson, J. W. (1972). On the post-buckling behavior of imperfection-sensitive structures in the plastic range. *J. Applied Mech.* **39**, 155–162.
Hutchinson, J. W. and Neale, K. W. (1977). Influence of strain-rate sensitivity on necking under uniaxial tension. *Acta Metallurgica* **25**, 839–846.
Hutchinson, J. W. and Obrecht, H. (1977). Tensile instabilities in strain-rate dependent materials. *Proc. Fourth International Congress on Fracture* (Edited by D. M. R. Taplin), pp. 101–116.
Hutchinson, J. W. and Tvergaard, V. (1981). Shear band formation in plane strain. *Int. J. Solids Structures* **17**, 451–470.
Leroy, Y. and Ortiz, M. (1989). Finite element analysis of strain localization in frictional materials. *Int. J. Numer. Anal. Meth. Geomech.* **13**, 53–74.
Leroy, Y. and Ortiz, M. (1990). Finite element analysis of transient strain localization phenomena in frictional solids. *Int. J. Numer. Anal. Meth. Geomech.* **14**, 93–124.
Leroy, Y., Needleman, A. and Ortiz, M. (1989). An overview of finite element methods for the analysis of strain localization. *Proc. France–U.S. Workshop on Strain Localization and Size Effect due to Cracking and Damage* (Edited by J. Mazars and Z. P. Bažant), Cachan.
Lubliner, J. (1964). A generalized theory of strain-rate-dependent plastic wave propagation in bars. *J. Mech. Phys. Solids* **12**, 59–65.
Mandel, J. (1971). *Plasticité Classique et Viscoplasticité*. Courses and lectures No. 97, CISM Udine. Springer, New York.
Marchand, A. and Duffy, J. (1988). An experimental study of the formation process of adiabatic shear bands in structural steel. *J. Mech. Phys. Solids* **36**, 251–283.
Molinari, A. (1988). Bandes de cisaillement dans un monocristal viscoplastique en traction simple. *C. R. Acad. Sci. Paris* **II**, 841–846.
Molinari, A. and Clifton, R. J. (1987). Analytical characterization of shear localization in thermoviscoplastic materials. *J. Applied Mech.* **54**, 806–812.
Nacar, A., Needleman, A. and Ortiz, M. (1989). A finite element method for analyzing localization in rate dependent solids at finite strains. *Comput. Meth. Appl. Mech. Engng* **73**, 235–258.
Needleman, A. (1988). Material rate dependence and mesh sensitivity in localization problems. *Comput. Meth. Appl. Mech. Engng* **67**, 69–85.
Nguyen, Q. S. (1984). Bifurcation et stabilité des systèmes irreversibles obéissant au principle de dissipation maximale. *J. de Mécanique* **3**, 41–61.
Ortiz, M., Leroy, Y. and Needleman, A. (1987). A finite element method for localized failure analysis. *Comput. Meth. Appl. Mech. Engng* **61**, 189–214.
Rabotnov, G. N. and Shesterikov, S. A. (1957). Creep stability of columns and plates. *J. Mech. Phys. Solids* **6**, 27–34.
Rice, J. R. (1970). On the structure of stress–strain relations for time-dependent plastic deformation in metals. *J. Applied Mech.* **37**, 728–737.
Rice, J. R. (1976). The localization of plastic deformation. In *Theoretical and Applied Mechanics* (Edited by W. T. Koiter), pp. 207–220. North-Holland, Amsterdam.
Riks, E. (1979). An incremental approach to the solution of snapping and buckling problems. *Int. J. Solids Structures* **15**, 529–551.
Sewell, M. J. (1965). The static perturbation technique in buckling problems. *J. Mech. Phys. Solids* **13**, 247–265.
Shanley, F. R. (1947). Inelastic column theory. *J. Aeronaut. Sci.* **14**, 261–268.
Triantafyllidis, N. (1980). Bifurcation phenomena in pure bending. *J. Mech. Phys. Solids* **28**, 221–245.
Tvergaard, V. (1982). Ductile fracture of cavity nucleation between larger voids. *J. Mech. Phys. Solids* **30**, 265–286.
Tvergaard, V. (1985). Rate-sensitivity in elastic-plastic panel buckling. In *Aspects of the Analysis of Plate Structures* (Edited by D. J. Darve *et al.*). Oxford.
Tvergaard, V., Needleman, A. and Lo, K. K. (1981). Flow localization in the plane strain tensile test. *J. Mech. Phys. Solids* **29**, 115–142.
Wilkinson, J. H. (1965). *The Algebraic Eigenvalue Problem*. Clarendon Press, Oxford.